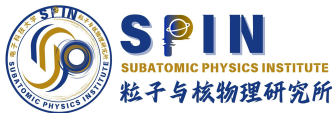


Probe Strongly Coupled Dark Sector via Gravitational Wave

Zhi-Wei Wang 王志伟

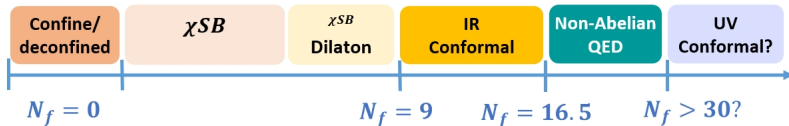
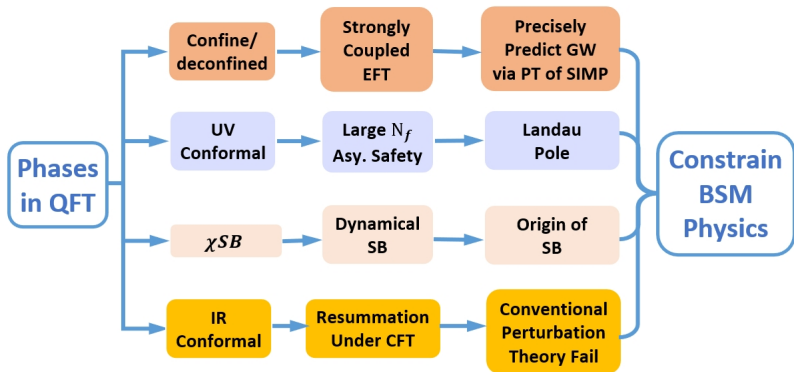
Uni. of Electronic Science and Technology of China

Oct. 25th, 2024



非微扰方法及其在高能物理中的应用专题研讨会
Oct. 25th - Oct. 27th 2024, 彭桓武高能基础理论研究中心 (合肥)

A Landscape of Phases in QFT and its Relation to BSM Physics

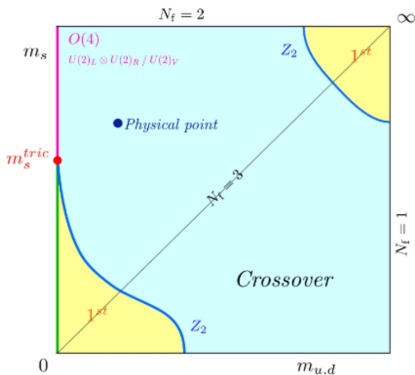
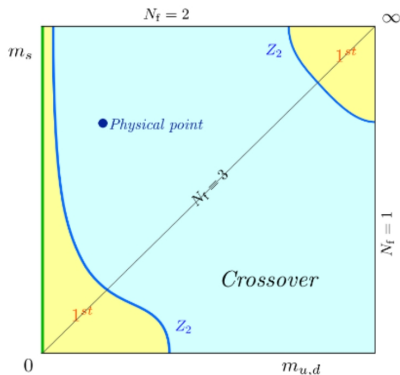


Motivations and what we do

- (Dark) composite dynamics: non perturbative physics, dynamical symmetry breaking, UV completion, naturalness
- (Dark) composite dynamics face challenges to be explored both theoretically and via experiments and thus any extra test is important
- We unify first principle lattice simulations and gravitational wave astronomy to constrain the dark sector

What composes the strongly coupled sector?

- Dark Yang-Mills theories
- Pure gluons \Rightarrow confinement-deconfinement phase transition
- Gluons + Fermions
 - Fermions in fundamental representation \Rightarrow chiral phase transition
 - Fermions in adjoint rep. \Rightarrow confinement & chiral phase transition
 - Fermions in 2-index symmetric rep. \Rightarrow confinement & chiral phase transition
- Gluons + Fermions + Scalars (not explored yet)



New Progresses in Columbia Plot

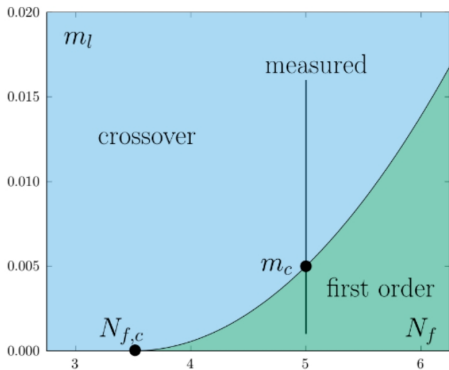
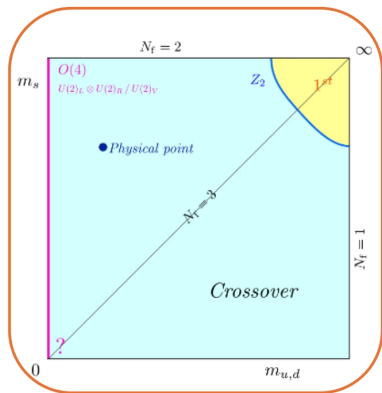


图: Left Fig. Columbia plot from JHEP 11 (2021) 141. Staggered fermions used. Right Fig. from PoS **LATTICE2022** (2023) 027.

How to describe the strongly coupled sector?

● Pure gluons

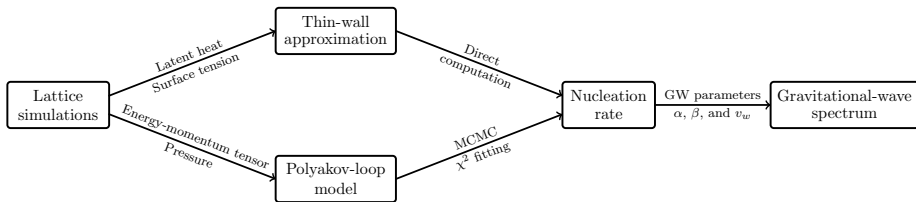
- **Polyakov loop model** (Huang, Reichert, Sannino and Z-W W, PRD **104** (2021) 035005; Kang, Zhu, Matsuzaki, JHEP 09 (2021) 060; Gao, Sun and White, arXiv:2405.00490.)
- **Matrix Model** (Halverson, Long, Maiti, Nelson, Salinas, JHEP **05** (2021) 154)
- **Holographic QCD model** (Ares, Henriksson, Hindmarsh, Hoyos, Jokela, PRD **105** (2022) 066020; Ares, Henriksson, Hindmarsh, Hoyos, Jokela, PRL **128** (2022) 131101)

● Gluons + Fermions

- **Polyakov loop improved Nambu-Jona-Lasinio model** (Reichert, Sannino, Z-W W and Zhang, JHEP **01** (2022) 003; Helmboldt, Kubo, Woude, PRD **100** (2019) 055025)
- **Linear sigma model** (Helmboldt, Kubo, Woude, PRD **100** (2019) 055025)
- **Polyakov Quark Meson model** (Pasechnik, Reichert, Sannino, Z-W W, JHEP **02** (2024) 159)

Procedure of pure gluon case

(Huang, Reichert, Sannino and Z-W W, PRD **104** (2021) 035005)



Polyakov Loop Model for Pure Gluons: I

- Pisarski first proposed the Polyakov-loop Model as an effective field theory to describe the confinement-deconfinement phase transition of $SU(N)$ gauge theory (Pisarski, PRD **62** (2000) 111501).
- In a local $SU(N)$ gauge theory, a **global center symmetry** $Z(N)$ is used to distinguish confinement phase (unbroken phase) and deconfinement phase (broken phase)
- An order parameter for the $Z(N)$ symmetry is constructed using the Polyakov Loop (thermal Wilson line) (Polyakov, PLB **72** (1978) 477)

$$\mathbf{L}(\vec{x}) = \mathcal{P} \exp \left[i \int_0^{1/T} A_4(\vec{x}, \tau) d\tau \right]$$

The symbol \mathcal{P} denotes path ordering and A_4 is the Euclidean temporal component of the gauge field

- The Polyakov Loop transforms like an adjoint field under local $SU(N)$ gauge transformations

Polyakov Loop Model for Pure Gluons: II

- Convenient to define the trace of the **Polyakov loop as an order parameter** for the $Z(N)$ symmetry

$$\ell(\vec{x}) = \frac{1}{N} \text{Tr}_c[\mathbf{L}],$$

where Tr_c denotes the trace in the colour space.

- Under a global $Z(N)$ transformation, the Polyakov loop ℓ transforms as a field with charge one

$$\ell \rightarrow e^{i\phi} \ell, \quad \phi = \frac{2\pi j}{N}, \quad j = 0, 1, \dots, (N-1)$$

- The expectation value of ℓ i.e. $\langle \ell \rangle$ has the **important property**:

$$\langle \ell \rangle = 0 \quad (T < T_c, \text{ Confined}); \quad \langle \ell \rangle > 0 \quad (T > T_c, \text{ Deconfined})$$

- At very high temperature, the vacua exhibit a N -fold degeneracy:

$$\langle \ell \rangle = \exp\left(i \frac{2\pi j}{N}\right) \ell_0, \quad j = 0, 1, \dots, (N-1)$$

where ℓ_0 is defined to be real and $\ell_0 \rightarrow 1$ as $T \rightarrow \infty$

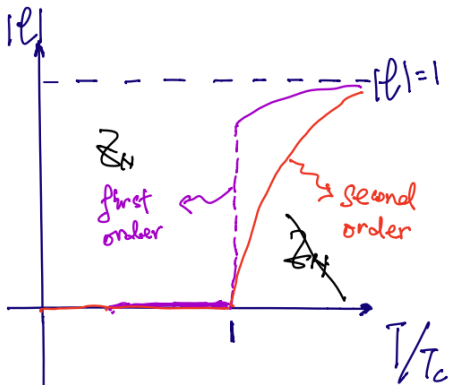
Summary of Pure Gluon Facts

Temperature

Free Gluon
 Z_N is broken

At $T_{\text{confinement}}$
Confinement
glue ball

Z_N is restored



Second Order for $SU(2)$
First order $SU(N)$ ($N \geq 3$)

EFT 1: Polyakov Loop Model

Effective Potential of the Polyakov Loop Model: I

- The simplest effective potential preserving the Z_N symmetry in the polynomial form is given by (Pisarski, PRD **62** (2000) 111501)

$$V_{\text{PLM}}^{(\text{poly})} = T^4 \left(-\frac{b_2(T)}{2} |\ell|^2 + b_4 |\ell|^4 + \dots - b_3 (\ell^N + \ell^{*N}) \right)$$

$$\text{where } b_2(T) = a_0 + a_1 \left(\frac{T_0}{T} \right) + a_2 \left(\frac{T_0}{T} \right)^2 + a_3 \left(\frac{T_0}{T} \right)^3 + a_4 \left(\frac{T_0}{T} \right)^4$$

"..." represent any required lower dimension operator than ℓ^N i.e. $(\ell\ell^*)^k = |\ell|^{2k}$ with $2k < N$.

- For the $SU(3)$ case, there is also an alternative logarithmic form

$$V_{\text{PLM}}^{(3\log)} = T^4 \left(-\frac{a(T)}{2} |\ell|^2 + b(T) \ln(1 - 6|\ell|^2 + 4(\ell^{*3} + \ell^3) - 3|\ell|^4) \right)$$

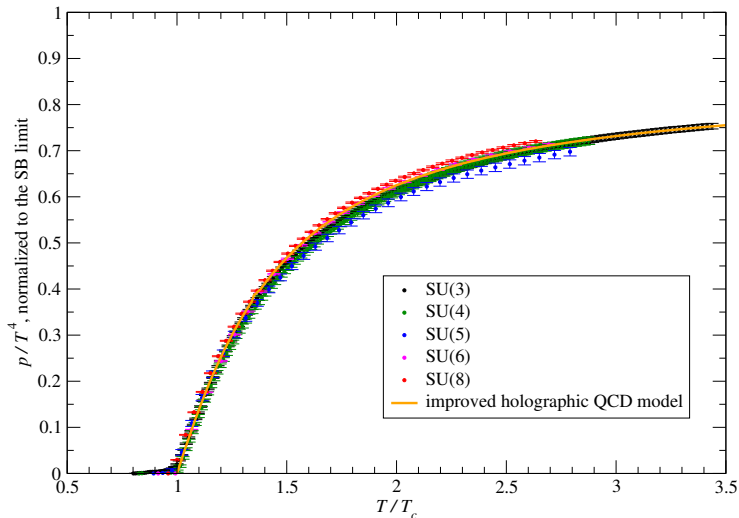
$$a(T) = a_0 + a_1 \left(\frac{T_0}{T} \right) + a_2 \left(\frac{T_0}{T} \right)^2 + a_3 \left(\frac{T_0}{T} \right)^3, \quad b(T) = b_3 \left(\frac{T_0}{T} \right)^3$$

- The a_i, b_i coefficients in $V_{\text{PLM}}^{(\text{poly})}$ and $V_{\text{PLM}}^{(3\log)}$ are determined by fitting the lattice results

Fitting the Coefficients Using the Lattice Results: I

Marco Panero, Phys.Rev.Lett. 103 (2009) 232001

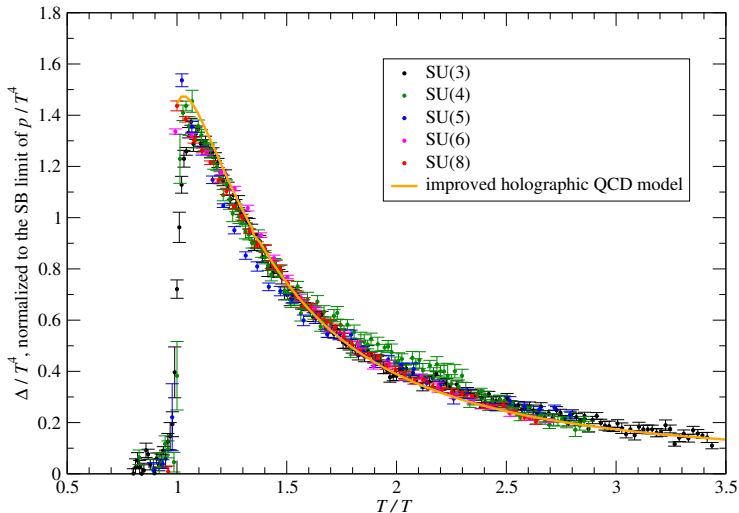
Pressure



Fitting the Coefficients Using the Lattice Results: II

Marco Panero, Phys.Rev.Lett. 103 (2009) 232001

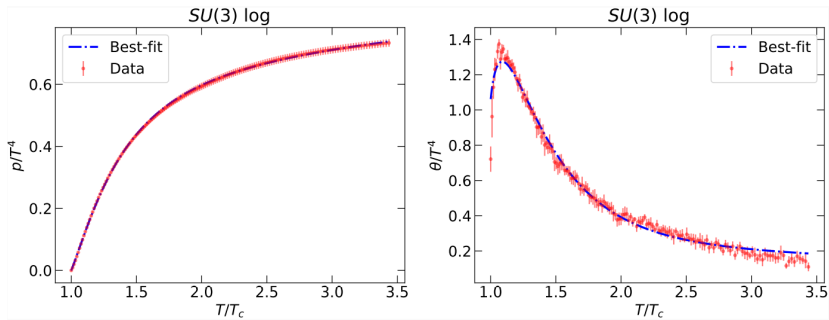
Trace of the energy-momentum tensor



Fitting the Coefficients Using the Lattice Results: III

(Huang, Reichert, Sannino and Z-W W, PRD **104** (2021) 035005)

Fitted to lattice data of pressure and the trace of energy momentum tensor.



Fitting the Coefficients Using the Lattice Results: IV

(Huang, Reichert, Sannino and Z-W W, PRD **104** (2021) 035005)

表: The parameters for the best-fit points.

N	3	3 log	4	5	6	8
a_0	3.72	4.26	9.51	14.3	16.6	28.7
a_1	-5.73	-6.53	-8.79	-14.2	-47.4	-69.8
a_2	8.49	22.8	10.1	6.40	108	134
a_3	-9.29	-4.10	-12.2	1.74	-147	-180
a_4	0.27		0.489	-10.1	51.9	56.1
b_3	2.40	-1.77		-5.61		
b_4	4.53		-2.46	-10.5	-54.8	-90.5
b_6			3.23		97.3	157
b_8					-43.5	-68.9

EFT 2: The PNJL Model

Include Fermions: the PNJL Model

(K. Fukushima, PLB **591** (2004) 277; Ratti, Thaler Weise, PRD **73** (2006) 014019)

Reichert, Sannino, Z-W W and Zhang, JHEP **01** (2022) 003, arXiv:2109.11552.

- The Polyakov-loop-Nambu-Jona-Lasinio (PNJL) model is used to describe phase-transition dynamics in dark gauge-fermion sectors
- The **finite-temperature grand potential** of the PNJL models can be generically written as

$$V_{\text{PNJL}} = V_{\text{PLM}}[\ell, \ell^*] + V_{\text{cond}}[\langle\bar{\psi}\psi\rangle] + V_{\text{zero}}[\langle\bar{\psi}\psi\rangle] + V_{\text{medium}}[\langle\bar{\psi}\psi\rangle, \ell, \ell^*]$$

- $V_{\text{PLM}}[\ell, \ell^*]$ is the Polyakov loop model potential (discussed above)
- $V_{\text{cond}}[\langle\bar{\psi}\psi\rangle]$ represents the condensate energy
- $V_{\text{zero}}[\langle\bar{\psi}\psi\rangle]$ denotes the fermion zero-point energy
- The medium potential $V_{\text{medium}}[\langle\bar{\psi}\psi\rangle, \ell, \ell^*]$ encodes the interactions between the chiral and gauge sector which arises from an integration over the quark fields coupled to a background gauge field

- The PNJL Lagrangian can be generically written as:

$$\mathcal{L}_{\text{PNJL}} = \mathcal{L}_{\text{pure-gauge}} + \mathcal{L}_{4\text{F}} + \mathcal{L}_{6\text{F}} + \mathcal{L}_k$$

- Without losing generality, we consider below massless 3-flavour case in fundamental representation of $SU(3)$ gauge symmetry
- Here, $\mathcal{L}_{4\text{F}}$ is the four-quark interaction which reads:

$$\mathcal{L}_{4\text{F}} = G_S \sum_{a=0}^8 [(\bar{\psi}\lambda^a\psi)^2 + (\bar{\psi}i\gamma^5\lambda^a\psi)^2], \quad \psi = (u, d, s)^T$$

- Six-fermion interaction $\mathcal{L}_{6\text{F}}$ denotes the Kobayashi-Maskawa-'t Hooft (KMT) term breaking $U(1)_A$ down to Z_3 (generically Z_{N_f} for N_f flavours)

$$\mathcal{L}_{6\text{F}} = G_D [\det(\bar{\psi}_{Li}\psi_{Rj}) + \det(\bar{\psi}_{Ri}\psi_{Lj})]$$

Medium Potential: Finite Temperature Contribution

- In the standard NJL model, the medium effect (finite temperature contribution) is implemented by the grand canonical partition function
- In the PNJL model, we can simply do the following replacement to include the contribution from Polyakov loop

$$V_{\text{medium}} = -2N_c T \sum_{u,d,s} \int \frac{d^3 p}{(2\pi)^3} \left(\ln \left[1 + e^{-\beta(E-\mu)} \right] + \ln \left[1 + e^{-\beta(E+\mu)} \right] \right)$$
$$\rightarrow -2T \sum_{u,d,s} \int \frac{d^3 p}{(2\pi)^3} \text{Tr}_c \left\{ \left(\ln \left[1 + \mathbf{L} e^{-\beta(E-\mu)} \right] + \ln \left[1 + \mathbf{L}^\dagger e^{-\beta(E+\mu)} \right] \right) \right\}$$

- \mathbf{L} is the Polyakov loop:

$$\mathbf{L}(\vec{x}) = \mathcal{P} \exp \left[i \int_0^{1/T} A_4(\vec{x}, \tau) d\tau \right]$$

- In this work, we consider chemical potential $\mu = 0$.

EFT 3: The PQM Model with CJT Method

Include Fermions: the PQM Model

(B. Schaefer, J. Pawłowski, J. Wambach PRD **76** (2007) 074023; B. Schaefer, M. Wagner, PNP **62** (2009) 391)

Pasechnik, Reichert, Sannino and Z-W W, JHEP **02** (2024) 159.

- The Polyakov quark meson model (PQM) is widely used as an effective theory to study the first order chiral phase transition
- The Lagrangian of the PLSM where mesons couple to a spatially constant temporal background gauge field reads

$$\mathcal{L} = \bar{q} (i\not{D} - g(\sigma + i\gamma_5 T^a \pi_a)) q + \frac{1}{2} (\partial_\mu \sigma)^2 + \frac{1}{2} (\partial_\mu \pi_a)^2 - V_{\text{PLM}}^{(\text{poly})} + V_{\text{LSM}} + V_{\text{medium}}, \text{ where } \not{D} = \gamma_\mu \partial_\mu - i\gamma_0 A_0$$

- V_{LSM} under symmetry $SU(N_f) \times SU(N_f)$ with N_f flavours reads

$$V_{\text{LSM}} = \frac{1}{2} (\lambda_\sigma - \lambda_a) \text{Tr}[\Phi^\dagger \Phi]^2 + \frac{N_f}{2} \lambda_a \text{Tr}[\Phi^\dagger \Phi \Phi^\dagger \Phi] - m^2 \text{Tr}[\Phi^\dagger \Phi] - 2(2N_f)^{N_f/2-2} c (\det \Phi^\dagger + \det \Phi)$$

where the meson field Φ is a $N_f \times N_f$ matrix defined as

$$\Phi = \frac{1}{\sqrt{2N_f}} (\sigma + i\eta') I + (a_a + i\pi_a) T^a, I \equiv \text{identity matrix}$$

The CJT Method: Concept and Advantages

(J. Cornwall, R. Jackiw, E. Tomboulis PRD 10 (1974) 2428; G. Amelino-Camelia, PRD 47 (1993) 2356)

Pasechnik, Reichert, Sannino and Z-W W, JHEP 02 (2024) 159.

- Cornwall, Jackiw and Tomboulis (CJT) first proposed a generalized effective action $\Gamma(\phi, G)$ of composite operators, where the effective action not only depends on $\phi(x)$ but also on the propagator $G(x, y)$
- The effective action becomes the generating functional of the two-particle irreducible (2PI) vacuum graphs rather than the conventional 1PI diagrams
- The CJT method is equivalent to summing up the infinite class of “daisy” and “super daisy” graphs and is thus useful in studying such strongly coupled models beyond mean-field approximation
- The PQM with the CJT method compared to other model computations such as holography and the PNJL model, can **bridge perturbative and non-perturbative regimes** of the effective theory

The CJT Method: Formalism

(J. Cornwall, R. Jackiw, E. Tomboulis PRD 10 (1974) 2428; G. Amelino-Camelia, PRD 47 (1993) 2356)

Pasechnik, Reichert, Sannino and Z-W W, arXiv:2309.16755.

- In CJT formalism, the finite temperature effective potential with generic scalar field ϕ is given by:

$$V_{\text{CJT}}(\phi, G) = V_0(\phi) + \frac{1}{2} \sum_i \int_{\beta} \ln G_i^{-1}(\phi; k) \\ + \frac{1}{2} \sum_i \int_{\beta} [D^{-1}(\phi; k)G(\phi; k) - 1] + V_2(\phi, G),$$

\sum_i runs over all meson species; $D^{-1}(\phi; k) \equiv$ tree level propagator
 $V_2(\phi, G) \equiv$ infinite sum of the two-particle irreducible vacuum graphs

- Using the Hartree approximation, $V_2(\phi, G)$ is simplified to a one “double bubble” diagram. In the simplest one-meson case, $V_2 \propto \left[\int_{\beta} G(\phi; k) \right]^2$.
- We therefore obtain a gap equation by minimizing the above effective potential with respect to the dressed propagator $G_i(\phi; k)$:

$$\frac{1}{2} G_i^{-1}(\phi; k) = \frac{1}{2} D_i^{-1}(\phi; k) + 2 \frac{\delta V_2(\phi, G)}{\delta G_i(\phi; k)}$$

The CJT Method: Formalism

(Pasechnik, Reichert, Sannino and Z-W W, arXiv:2309.16755.)

- Using the gapped equation, the thermal mass is given by ($R_i \equiv M_i/T$):

$$M_\sigma^2 = m_\sigma^2 + \frac{T^2}{4\pi^2} \left[\left(3\lambda_\sigma - \delta_{4,N_f} \frac{3}{2}c \right) I_B(R_\sigma) \right. \\ \left. + \left((N_f^2 - 1)(\lambda_\sigma + 2\lambda_a) + \delta_{4,N_f} \frac{15}{2}c \right) I_B(R_a) \right. \\ \left. + \left(\lambda_\sigma + \delta_{4,N_f} \frac{3}{2}c \right) I_B(R_\eta) + \left((N_f^2 - 1)\lambda_\sigma - \delta_{4,N_f} \frac{15}{2}c \right) I_B(R_\pi) \right],$$

- CJT improved finite temperature effective potential:

$$V_{\text{FT}}^{\text{LSM}}(\sigma) = \frac{T^4}{2\pi^2} \sum_i \left[J_B(R_i^2) - \frac{1}{4} (R_i^2 - r_i^2) I_B(R_i^2) \right],$$

$$I_B(R^2) = 2 \frac{dJ_B(R^2)}{dR^2} = \int_0^\infty dx \frac{x^2}{\sqrt{x^2 + R^2}} \frac{1}{e^{\sqrt{x^2 + R^2}} - 1},$$

$$J_B(R^2) = \int_0^\infty dx x^2 \ln \left(1 - e^{-\sqrt{x^2 + R^2}} \right).$$

Second Part: Bubble Nucleation and Gravitational Wave

Bubble Nucleation: Generic Discussion

- In a first-order phase transition, the transition occurs via bubble nucleation and it is essential to compute the nucleation rate
- The tunnelling rate due to thermal fluctuations from the metastable vacuum to the stable one is suppressed by the three-dimensional Euclidean action $S_3(T)$

$$\Gamma(T) = T^4 \left(\frac{S_3(T)}{2\pi T} \right)^{3/2} e^{-S_3(T)/T}$$

- The generic three-dimensional Euclidean action reads

$$S_3(T) = 4\pi \int_0^\infty dr r^2 \left[\frac{1}{2} \left(\frac{d\rho}{dr} \right)^2 + V_{\text{eff}}(\rho, T) \right],$$

where ρ denotes a generic scalar field with mass dimension one, $[\rho] = 1$

Bubble Nucleation: Confinement Phase Trans. (PLM)

(Huang, Reichert, Sannino and Z-W W, PRD **104** (2021) 035005)

- Confinement phase transition occurs for pure gluon and adjoint fermions
- $[\ell] = 0$ dimensionless while $[\rho] = 1$, we rewrite ρ as $\rho = \ell T$ and convert the radius into a dimensionless quantity $r' = r T$:

$$S_3(T) = 4\pi T \int_0^\infty dr' r'^2 \left[\frac{1}{2} \left(\frac{d\ell}{dr'} \right)^2 + V'_{\text{eff}}(\ell, T) \right],$$

which has the same form as the above generic equation.

- The bubble profile (instanton solution) is obtained by solving the E.O.M. of the $S_3(T)$

$$\frac{d^2\ell(r')}{dr'^2} + \frac{2}{r'} \frac{d\ell(r')}{dr'} - \frac{\partial V'_{\text{eff}}(\ell, T)}{\partial \ell} = 0$$

- The boundary conditions (deconfinement \rightarrow confinement) are

$$\frac{d\ell(r' = 0, T)}{dr'} = 0, \quad \lim_{r' \rightarrow 0} \ell(r', T) = 0$$

- We used the method of overshooting/undershooting (Python package)

Bubble Profile of Confinement Phase Transition

(Huang, Reichert, Sannino and Z-W W, PRD **104** (2021) 035005)

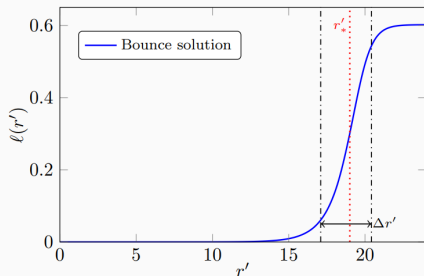
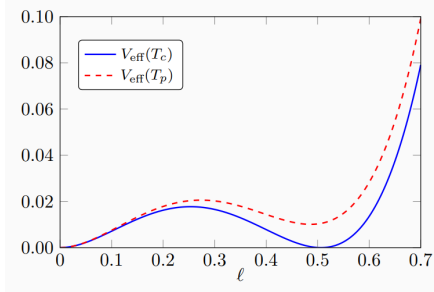


图: The bubble radius is indicated by r'_* and the wall width by $\Delta r'$. Inside of the bubble ($r' \ll r'_*$) lying the **confinement phase**, the Z_N symmetry is unbroken and $\langle \ell \rangle = 0$, while outside of the bubble ($r \gg r'_*$) lying the **deconfinement phase**, the Z_N symmetry is broken and $\langle \ell \rangle > 0$.

Bubble Nucleation: Chiral Phase Transition (PNJL)

(Reichert, Sannino, Z-W W and Zhang, JHEP 01 (2022) 003, arXiv:2109.11552)

- Chiral phase transition occurs when including fermions
- $\bar{\sigma}$ is classically nonpropagating in PNJL and it's kinetic term is induced only via quantum fluctuations
- We thus include its wave-function renormalization Z_σ with

$$Z_\sigma^{-1} = - \left. \frac{d\Gamma_{\sigma\sigma}(q^0, \mathbf{q}, \bar{\sigma})}{d\mathbf{q}^2} \right|_{q^0=0, \mathbf{q}^2=0}, \quad \Gamma_{\sigma\sigma} = -i \sum \text{2 point 1PI } \sigma\sigma \text{ graph}$$

- The three-dimensional Euclidean action and E.O.M. are modified to:

$$S_3(T) = 4\pi \int_0^\infty dr r^2 \left[\frac{Z_\sigma^{-1}}{2} \left(\frac{d\bar{\sigma}}{dr} \right)^2 + V_{\text{eff}}(\bar{\sigma}, T) \right]$$

$$\frac{d^2\bar{\sigma}}{dr^2} + \frac{2}{r} \frac{d\bar{\sigma}}{dr} - \frac{1}{2} \frac{\partial \log Z_\sigma}{\partial \bar{\sigma}} \left(\frac{d\bar{\sigma}}{dr} \right)^2 = Z_\sigma \frac{\partial V_{\text{eff}}}{\partial \bar{\sigma}}$$

- The associated boundary conditions:

$$\frac{d\bar{\sigma}(r=0, T)}{dr} = 0, \quad \lim_{r \rightarrow \infty} \bar{\sigma}(r, T) = 0$$

Gravitational Wave Parameters: Inverse Duration Time

- The phase-transition temperature T_* is often identified with the nucleation temperature T_n defined as the temperature where the rate of bubble nucleation per Hubble volume and time is order one: $\Gamma/H^4 \sim \mathcal{O}(1)$
- More accurately, we can use **percolation temperature** T_p : the temperature at which 34% of false vacuum is converted
- For sufficiently fast phase transitions, the decay rate is approximated by:

$$\Gamma(T) \approx \Gamma(t_*)e^{\beta(t-t_*)}$$

- The inverse duration time then follows as

$$\beta = -\left. \frac{d}{dt} \frac{S_3(T)}{T} \right|_{t=t_*}$$

- The dimensionless version $\tilde{\beta}$ is defined relative to the Hubble parameter H_* at the characteristic time t_*

$$\tilde{\beta} = \frac{\beta}{H_*} = T \left. \frac{d}{dT} \frac{S_3(T)}{T} \right|_{T=T_*},$$

where we used that $dT/dt = -H(T)T$.

Gravitational Wave Parameters: Strength Parameter I

(Huang, Reichert, Sannino and Z-W W, PRD **104** (2021) 035005)

Reichert, Sannino, Z-W W and Zhang, JHEP **01** (2022)003, arXiv:2109.11552.)

- We define the strength parameter α from the **trace of the energy-momentum tensor** θ weighted by the enthalpy

$$\alpha = \frac{1}{3} \frac{\Delta\theta}{w_+} = \frac{1}{3} \frac{\Delta e - 3\Delta p}{w_+}, \quad \Delta X = X^{(+)} - X^{(-)}, \text{ for } X = (\theta, e, p)$$

(+) denotes the meta-stable phase (outside of the bubble) while (-) denotes the stable phase (inside of the bubble).

- The relations between enthalpy w , pressure p , and energy e are given by

$$w = \frac{\partial p}{\partial \ln T}, \quad e = \frac{\partial p}{\partial \ln T} - p,$$

which are extracted from the effective potential with

$$p^{(\pm)} = -V_{\text{eff}}^{(\pm)}$$

Gravitational Wave Parameters: Strength Parameter II

(Huang, Reichert, Sannino and Z-W W, PRD **104** (2021) 035005

Reichert, Sannino, Z-W W and Zhang, JHEP **01** (2022) 003, arXiv:2109.11552.)

- α is thus given by

$$\alpha = \frac{1}{3} \frac{4\Delta V_{\text{eff}} - T \frac{\partial \Delta V_{\text{eff}}}{\partial T}}{-T \frac{\partial V_{\text{eff}}^{(+)}}{\partial T}},$$

- For confinement phase transition: $\alpha \approx 1/3$ (ΔV_{eff} is negligible since $e_+ \gg p_+$ and $e_- \sim p_- \sim 0$ in PLM potential)
- For chiral phase transition: we find smaller values, $\alpha \sim \mathcal{O}(10^{-2})$, due to the fact that more relativistic d.o.f.s participate in the phase transition
- Relativistic SM d.o.f.s do not contribute to our definition of α since they are fully decoupled from the phase transition but these d.o.f.s will play a role to dilute the GW signals

GW parameters α , β and PNJL observables

(Reichert, Sannino, Z-W W and Zhang, JHEP 01 (2022) 003, arXiv:2109.11552.)

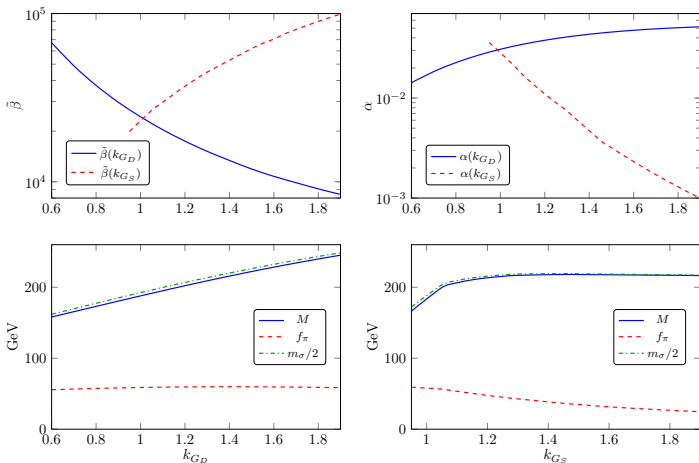


图: The GW parameters $\tilde{\beta}$, α with the observables M , f_π , and m_σ as a function of $G_S = k_{G_S} \cdot 4.6 \text{ GeV}^{-2}$ and $G_D = k_{G_D} \cdot (-743 \text{ GeV}^{-5})$. We use $T_c = 100 \text{ GeV}$, the ratio $\Lambda/T_0 = 3.54$. Below $k_{G_S, \text{crit}} = 0.882$, no chiral symmetry breaking occurs.

Gravitational-wave spectrum

(Huang, Reichert, Sannino and Z-W W, PRD **104** (2021) 035005)

- Contributions from bubble collision and turbulence are subleading
- The GW spectrum from sound waves is given by

$$h^2 \Omega_{\text{GW}}(f) = h^2 \Omega_{\text{GW}}^{\text{peak}} \left(\frac{f}{f_{\text{peak}}} \right)^3 \left[\frac{4}{7} + \frac{3}{7} \left(\frac{f}{f_{\text{peak}}} \right)^2 \right]^{-\frac{7}{2}}$$

- The peak frequency

$$f_{\text{peak}} \simeq 1.9 \cdot 10^{-5} \text{ Hz} \left(\frac{g_*}{100} \right)^{\frac{1}{6}} \left(\frac{T}{100 \text{ GeV}} \right) \left(\frac{\tilde{\beta}}{v_w} \right)$$

- The peak amplitude

$$h^2 \Omega_{\text{GW}}^{\text{peak}} \simeq 2.65 \cdot 10^{-6} \left(\frac{v_w}{\tilde{\beta}} \right) \left(\frac{\kappa_{sw} \alpha}{1 + \alpha} \right)^2 \left(\frac{100}{g_*} \right)^{\frac{1}{3}} \Omega_{\text{dark}}^2$$

- The factor Ω_{dark}^2 accounts for the dilution of the GWs by the non-participating SM d.o.f.

$$\Omega_{\text{dark}} = \frac{\rho_{\text{rad,dark}}}{\rho_{\text{rad,tot}}} = \frac{g_{*,\text{dark}}}{g_{*,\text{dark}} + g_{*,\text{SM}}}$$

The Efficiency Factor κ

- The efficiency factor for the sound waves κ_{SW} consist of κ_v as well as an additional suppression due to the length of the sound-wave period τ_{SW}

$$\kappa_{\text{SW}} = \sqrt{\tau_{\text{SW}}} \kappa_v$$

- τ_{SW} is dimensionless and measured in units of the Hubble time (H.-K. Guo, Sinha, Vagie and White, JCAP **01** (2021) 001)

$$\tau_{\text{SW}} = 1 - 1/\sqrt{1 + 2\frac{(8\pi)^{\frac{1}{3}}v_w}{\tilde{\beta}\bar{U}_f}} \Rightarrow \tau_{\text{SW}} \sim \frac{(8\pi)^{\frac{1}{3}}v_w}{\tilde{\beta}\bar{U}_f} \text{ for } \beta \gg 1$$

where \bar{U}_f is the root-mean-square fluid velocity

$$\bar{U}_f^2 = \frac{3}{v_w(1+\alpha)} \int_{c_s}^{v_w} d\xi \xi^2 \frac{v(\xi)^2}{1-v(\xi)^2} \simeq \frac{3}{4} \frac{\alpha}{1+\alpha} \kappa_v$$

- τ_{SW} is suppressed for large β occurring often in strongly coupled sectors
- κ_v was numerically fitted to simulation results depends α and v_w . At the Chapman-Jouguet detonation velocity it reads

$$\kappa_v(v_w = v_J) = \frac{\sqrt{\alpha}}{0.135 + \sqrt{0.98 + \alpha}}$$

GW Signatures for Arbitrary N in the Pure Gluon Case

(Huang, Reichert, Sannino and Z-W W, PRD **104** (2021) 035005)

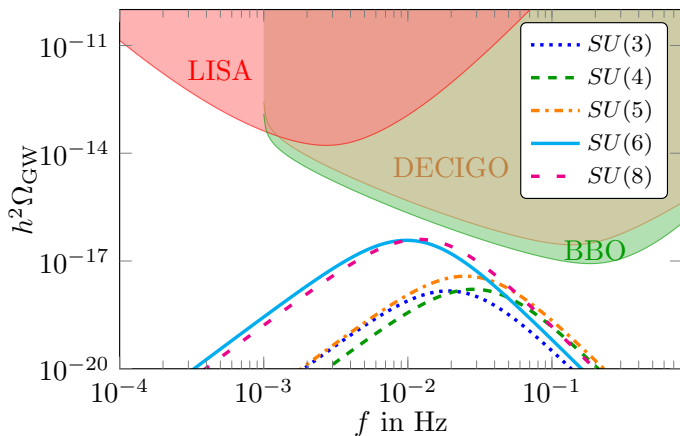


图: The dependence of the GW spectrum on the number of dark colours is shown for the values $N = 3, 4, 5, 6, 8$. All spectra are plotted with the bubble wall velocity set to the Chapman-Jouguet detonation velocity and with $T_c = 1$ GeV.

A Landscape of GW Signatures with Pure Gluon

(Huang, Reichert, Sannino and Z-WW, PRD **104** (2021) 035005)

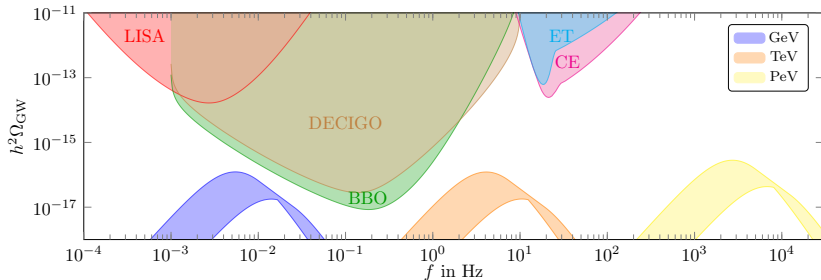


图: We display the GW spectrum of the $SU(6)$ phase transition for different confinement scales including $T_c = 1$ GeV, 1 TeV, and 1 PeV. We compare it to the power-law integrated sensitivity curves of LISA, BBO, DECIGO, CE, and ET.

Signal to Noise Ratio

(Huang, Reichert, Sannino and Z-W W, PRD **104** (2021) 035005)

$$\text{SNR} = \sqrt{\frac{3\text{year}}{s} \int_{f_{\min}}^{f_{\max}} df \left(\frac{h^2 \Omega_{\text{GW}}}{h^2 \Omega_{\text{det}}} \right)^2}$$

$h^2 \Omega_{\text{GW}}$ is the GW spectrum while Ω_{det} is the sensitivity curve of the detector.

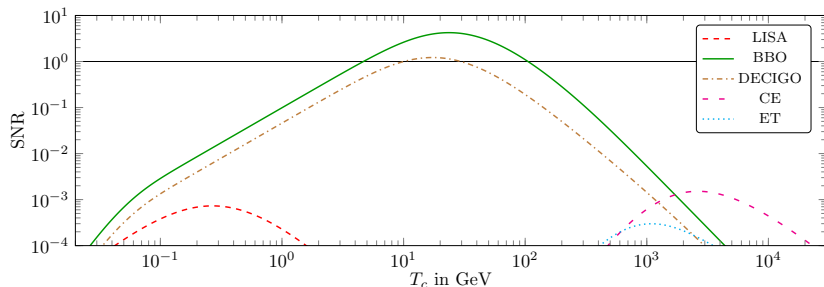


图: We display the SNR for the phase transition in a dark $SU(6)$ sector as a function of the confinement temperature T_c from experiments of LISA, BBO, DECIGO, CE, and ET. We assume an observation time of three years.

Landscape of GW spectrum with three Dirac fermions

(Reichert, Sannino, Z-W W and Zhang, JHEP 01 (2022) 003, arXiv:2109.11552.)

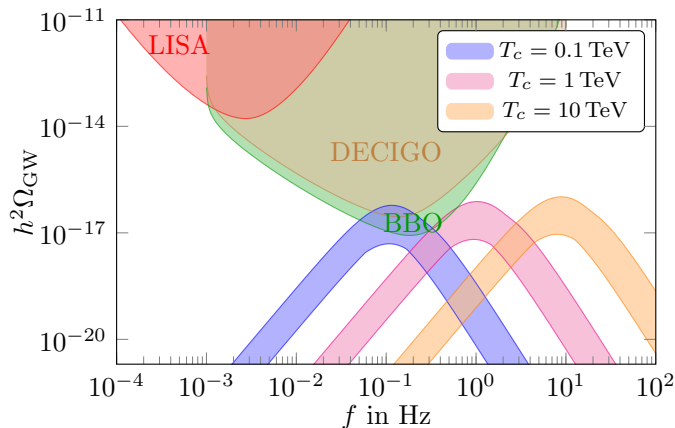


图: Gravitational-wave spectrum with three Dirac fermions in the fundamental representation for different critical temperatures. The band comes from varying wall velocity $c_s \leq v_w \leq 1$.

Representation Matters

(Reichert, Sannino, Z-W W and Zhang, JHEP 01 (2022) 003, arXiv:2109.11552.)

Rep.	flavour	chiral PT	conf.-deconf.
Fund.	3	1st	X
adjoint	1	2nd	1st
2-index Sym.	1	2nd	1st

表: Representations versus different phase transitions.

- Need small N_f to remain below the conformal Banks-Zaks window ($N_f \leq 2$ for adjoint and $N_f \leq 3$ for 2-index symmetric under $SU(3)$).

Signal to Noise Ratio for Different Representations

(Reichert, Sannino, Z-W W and Zhang, JHEP 01 (2022) 003, arXiv:2109.11552.)

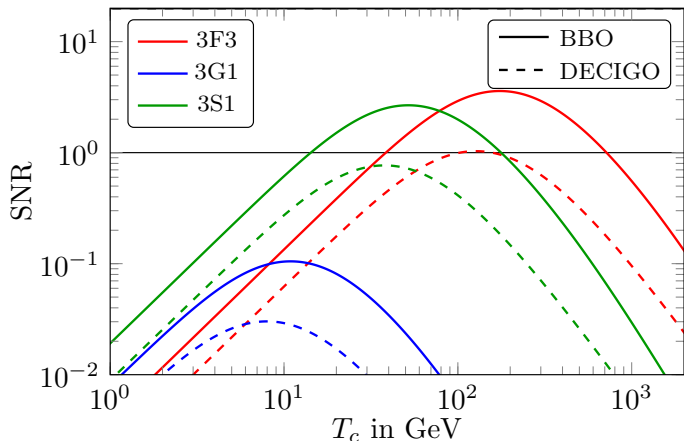


图: Signal-to-noise ratio as a function of the critical temperature for the best-case scenarios of each model at BBO and DECIGO with an observation time of 3 years.

Understanding from Thin Wall Approximation

- The three-dimensional Euclidean action S_3 can be written as a function of the latent heat L and the surface tension σ

$$S_3 = \frac{16\pi}{3} \frac{\sigma(T_c)^3}{L(T_c)^2} \frac{T_c^2}{(T_c - T)^2},$$

- The ratio $S_3(T_p)/T_p$ is typically a number $\mathcal{O}(150)$ for phase transitions around the electroweak scale and the inverse duration $\tilde{\beta}$ follows as

$$\tilde{\beta} = T \left. \frac{d}{dT} \frac{S_3(T)}{T} \right|_{T=T_p} \approx \mathcal{O}(10^3) \frac{T_c^{1/2} L}{\sigma^{3/2}}.$$

- $\tilde{\beta}$ stems from the competition between the surface tension and latent heat. $L \sim N^2$ while σ can be either $\sigma \sim N$ or $\sigma \sim N^2$ with limited data up to $SU(8)$
- How to construct models with smaller latent heat and larger surface tension to enhance the gravitational wave signals?

$\alpha - \beta$ Phase diagram via PQM Model

(Pasechnik, Reichert, Sannino and Z-W W, JHEP 02 (2024) 159.)

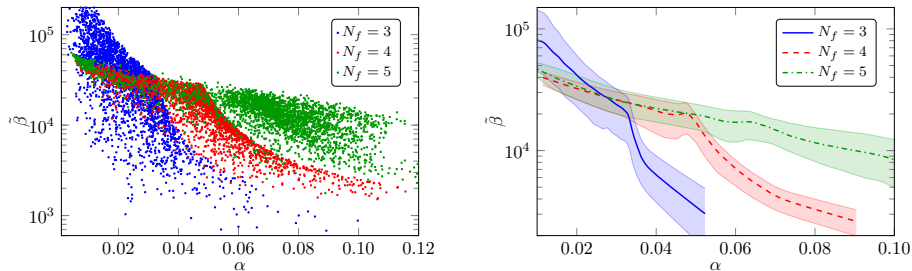


图: We show the range of α and $\tilde{\beta}$ values of the LSM for $N_f = 3, 4, 5$. In the left panel, we show the actual distribution of theory points, while in the right panel, we display the averaged values. On average, the LSM produces stronger GW signals with increasing N_f due to the larger α values. Nonetheless, the strongest GW signals are achieved with the LSM for $N_f = 3$, corresponding to the sparse blue dots at small $\tilde{\beta}$ in the left panel.

Strongest GW Signal at Small $m_\sigma \rightarrow$ Near Conformal

(Pasechnik, Reichert, Sannino and Z-W W, JHEP 02 (2024) 159.)

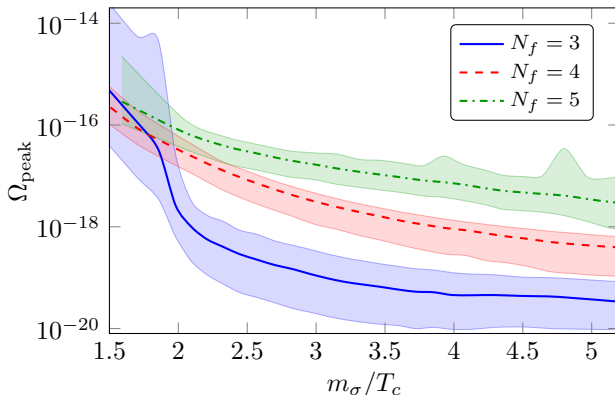


图: We show the averaged values of the peak amplitude Ω_{peak} as a function of physical observables m_σ in units of T_c in the LSM for $N_f = 3, 4, 5$. The sigma meson mass has the strong correlation with the peak amplitude: smaller values of m_σ lead to a larger Ω_{peak} . **The strongest signal can almost reach LISA sensitivity.**

Third Part: Glueball Dark Matter Production Mechanism

Rigorous Dark Gluon-gluon Dynamics

(Carenza, Pasechnik, Salinas, Z-W W, Phys. Rev. Lett. **129** (2022) no.26, 26)

- In the literature, for glueball dark matter production, only ϕ^5 interaction is considered, making the $3 \rightarrow 2$ annihilation the only relevant process for DM formation
- However, since glueball is strongly coupled, this naive calculation is not rigorous. **A non-perturbative method is required.**
- The dark gluon-gluon dynamics can be effectively described by considering the dimension-4 glueball field $\mathcal{H} \propto \text{tr}(G^{\mu\nu} G_{\mu\nu})$:

$$V[\mathcal{H}, \ell] = \frac{\mathcal{H}}{2} \ln \left[\frac{\mathcal{H}}{\Lambda^4} \right] + T^4 \mathcal{V}[\ell] + \mathcal{H} \mathcal{P}[\ell] + V_T[\mathcal{H}].$$

- To canonically normalize this field, we introduce ϕ as $\mathcal{H} = 2^{-8} c^{-2} \phi^4$
- We keep the lowest order in $\mathcal{P}[\ell]$ to satisfy the symmetry:

$$\mathcal{P}[\ell] = c_1 |\ell|^2,$$

where c_1 is determined by the lattice results (**jumping of gluon condensate**).

Cosmological evolution of the dark glueball field

(Carenza, Pasechnik, Salinas, Z-W W, Phys. Rev. Lett. 129 (2022) no.26, 26)

- The glueball field is considered homogeneous and evolves in expanding FLRW universe, with the E.O.M.

$$\ddot{\phi} + 3H\dot{\phi} + \partial_{\phi}V[\phi, T] = 0,$$

- The time variable is found in terms of the photon temperature:

$$t = \frac{1}{2} \sqrt{\frac{45}{4\pi^3 g_{*,\rho}(T_{\gamma})}} \frac{m_P}{T_{\gamma}^2}, \quad T_{\gamma} = \xi_T T$$

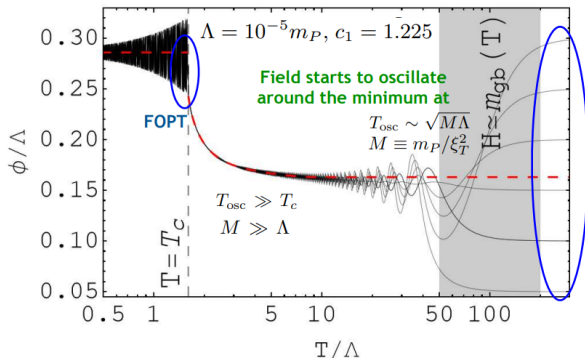
where ξ_T denotes the visible-to-dark sector temperature ratio and $m_P = 1.22 \times 10^{19}$ GeV is the Planck mass and $g_{*,\rho}$ is the number of energy-related degrees of freedom.

- E.O.M. in terms of the dark sector temperature:

$$\frac{4\pi^3 g_{*,\rho}}{45m_P^2} \xi_T^4 T^6 \frac{d^2\phi}{dT^2} + \frac{2\pi^3}{45m_P^2} \frac{dg_{*,\rho}}{dT} \xi_T^4 T^6 \frac{d\phi}{dT} + \partial_{\phi}V[\phi, T] = 0$$

Cosmological Evolution of the Dark Glueball Field

(Carenza, Pasechnik, Salinas, Z-W W, Phys. Rev. Lett. **129** (2022) no.26, 26)



- Field starts to oscillate around the minimum of the potential when $H \simeq m_{\text{gb}}$ with temperature $T_{\text{OSC}} \sim \sqrt{M\Lambda}$
- In early times in deconfined regime, for different initial conditions the field evolution follows the minimum (red dashed line).
- First order phase transition washes out any dependence on initial conditions.

Glueball Relic Density

(Carenza, Pasechnik, Salinas, Z-W W, Phys. Rev. Lett. **129** (2022) no.26, 26)

- Energy stored in these oscillations around $\phi_{\min} \approx 0.28\Lambda$ is the relic DM abundance, $\Omega h^2 = \rho/\rho_c$ (critical density $\rho_c = 1.05 \times 10^4 \text{ eV cm}^{-3}$)

$$\rho = \frac{2\pi^3}{45} g_{*,\rho}(T) \frac{T^6}{M^2} \left(\frac{d\phi}{dT} \right)^2 + V[\phi].$$

- Then the relic density today is calculated:

$$\Omega h^2 = \frac{\Lambda}{\rho_c/h^2} \left\langle \frac{\tilde{\rho}}{\tilde{T}^3} \right\rangle_f T_f^3 \left(\frac{T_{\gamma,0}}{\zeta_T T_f} \right)^3 = 0.12 \zeta_T^{-3} \frac{\Lambda}{\Lambda_0},$$

with dilution factor $(T_{\gamma,0}/\zeta_T T_f)^3$ to consider the Universe expansion

- Below freeze-out temperature, the predicted glueball relic density is

$$0.12 \zeta_T^{-3} \frac{\Lambda}{137.9 \text{ eV}} \lesssim \Omega h^2 \lesssim 0.12 \zeta_T^{-3} \frac{\Lambda}{82.7 \text{ eV}}, \quad 1.035 < c_1 < 1.415$$

for $\zeta_T^{-1} = 0.1$, the glueball dark matter mass is $\sim 100 \text{ MeV}$

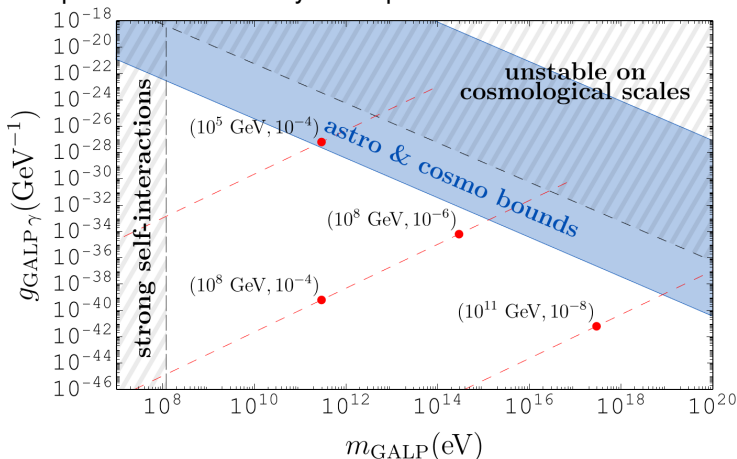
- It is more than a factor of 10 difference compared to the old calculations

$$\Omega h^2 \sim 0.12 \zeta_T^{-3} \frac{\Lambda}{5.45 \text{ eV}}$$

Further Progresses: Glueball as Axion-like Particle

(Carenza, Pasechnik, Z-W W, arXiv: 2408.14245)

- We further generalize the system to incorporate both 0^{++} and excited state 0^{-+} of glueball
- The glueball may play a role as an axion-like particle with much larger mass compared to the ordinary axion particle





已有成员



杜孟林 教授

研究方向：
强子物理与强相互作用、
中高能核物理



王志伟 研究员

研究方向：
粒子物理唯象、超出
标准模型的新物理



刘晓 教授

研究方向：
量子场论与弦论



杨智 研究员

研究方向：
强子物理与强相互作用、
中高能核物理



王金伟 副教授

研究方向：
暗物质唯象、超出标
准模型的新物理



Francesco Sannino

丹麦皇家科学院院士与芬兰科学院院士、
电子科技大学名誉教授

研究方向：粒子物理理论与唯象学，超越
标准模型的新物理，量子场论



金晟洙 研究员

研究方向：
量子场论与弦论

Thank you for your attention!

About Center Symmetry and Confinement

- The standard physical interpretation is that it is related to the free energy of adding an external static color source in the fundamental representation.

$$\ell(\vec{x}) = \exp(-F\beta)$$

- In the confinement phase, Polyakov loop is zero corresponds to infinity free energy to add a color source and the same time center symmetry is unbroken.

Center Symmetry $Z(N)$ at Nonzero Temperature

- The boundary conditions in imaginary time τ the fields must satisfy are:

$$A_\mu(\vec{x}, \beta) = +A_\mu(\vec{x}, 0), \quad q(\vec{x}, \beta) = -q(\vec{x}, 0),$$

where gluons as bosons must be periodic in τ while quarks as fermions must be anti-periodic.

- 't Hooft first noticed that one can consider more general gauge transformations which are only periodic up to Ω_c

$$\Omega(\vec{x}, \beta) = \Omega_c, \quad \Omega(\vec{x}, 0) = 1 \quad \left(\text{here, } \Omega_c = e^{i\phi} I, \phi = \frac{2\pi j}{N} \right).$$

- Color adjoint fields are invariant under this transformation, while those in the fundamental representation are not:

$$A_\mu^\Omega(\vec{x}, \beta) = \Omega_c^\dagger A_\mu(\vec{x}, \beta) \Omega_c = A_\mu(\vec{x}, \beta) = +A_\mu(\vec{x}, 0),$$

$$q^\Omega(\vec{x}, \beta) = \Omega_c^\dagger q(\vec{x}, \beta) = e^{-i\phi} q(\vec{x}, \beta) \neq -q(\vec{x}, 0).$$

- Thermal Wilson line transforms like an adjoint field under local $SU(N)$ gauge transformations:

$$L(x) \rightarrow \Omega^\dagger(\vec{x}, \beta) L(\vec{x}) \Omega^\dagger(\vec{x}, 0).$$

The Constituent Quark Mass and Zero Point Energy: I

(Fukushima, Skokov, PPNP 96 (2017) 154)

- In \mathcal{L}_{6F} , there is also $\langle \bar{u}u \rangle^2 \bar{u}u$ term contributes to the constituent quark mass of u
- The total constituent quark mass from \mathcal{L}_{4F} and \mathcal{L}_{6F} is:

$$M = -4G_S\sigma - \frac{1}{4}G_D\sigma^2$$

- The expression for the zero-point energy is given by:

$$V_{\text{zero}}[\langle \bar{\psi}\psi \rangle] = -\dim(\mathbb{R}) 2N_f \int \frac{d^3p}{(2\pi)^3} E_p, \quad E_p = \sqrt{\vec{p}^2 + M^2}$$

E_p is the energy of a free quark with constituent mass M and three-momentum \vec{p}

- The above integration diverges and a regularization is required. We choose a sharp three-momentum cutoff Λ entering the expression for observables and thus also a parameter of the theory.
- Parameters: G_S, G_D, Λ ; Observables: M, f_π, m_σ

The Constituent Quark Mass and Zero Point Energy: II

(Fukushima, Skokov, PPNP **96** (2017) 154)

- The integration can be carried analytically and the result is:

$$V_{\text{zero}}[\langle\bar{\psi}\psi\rangle] = -\frac{\dim(\mathbf{R})N_f\Lambda^4}{8\pi^2} \left[(2 + \xi^2)\sqrt{1 + \xi^2} + \frac{\xi^4}{2} \ln \frac{\sqrt{1 + \xi^2} - 1}{\sqrt{1 + \xi^2} + 1} \right],$$

in which $\xi \equiv \frac{M}{\Lambda}$.

- In \mathcal{L}_{4F} , the condensate energy then comes from the combination

$$(\bar{\psi}\lambda^0\psi)^2 + (\bar{\psi}\lambda^3\psi)^2 + (\bar{\psi}\lambda^8\psi)^2 = 2(\bar{u}u)^2 + 2(\bar{d}d)^2 + 2(\bar{s}s)^2$$

- We use the trick is to rewrite $(\bar{u}u)^2$ as

$$\begin{aligned}(\bar{u}u)^2 &= [(\bar{u}u - \langle\bar{u}u\rangle) + \langle\bar{u}u\rangle]^2 = (\bar{u}u - \langle\bar{u}u\rangle)^2 + 2\langle\bar{u}u\rangle(\bar{u}u - \langle\bar{u}u\rangle) + \langle\bar{u}u\rangle^2 \\ &\simeq -\langle\bar{u}u\rangle^2 + 2\langle\bar{u}u\rangle\bar{u}u,\end{aligned}$$

where the $(\bar{u}u - \langle\bar{u}u\rangle)^2$ term is dropped in the spirit of the **mean-field approximation**.

- The $2\langle\bar{u}u\rangle\bar{u}u$ term contributes to the constituent quark mass of u
- The $-\langle\bar{u}u\rangle^2$ term leads to a contribution to the condensate energy
- Similar procedures can be applied to $(\bar{d}d)^2$ and $(\bar{s}s)^2$, and to \mathcal{L}_{6F} gives $\langle\bar{u}u\rangle^3$ and we obtain the total condensate energy:

$$V_{\text{cond}} = 6G_S\sigma^2 + \frac{1}{2}G_D\sigma^3, \quad \sigma \equiv \langle\bar{u}u\rangle = \langle\bar{d}d\rangle = \langle\bar{s}s\rangle = \frac{1}{3}\langle\bar{\psi}\psi\rangle$$

About Thin Wall Approximation

The three-dimensional Euclidean action S_3 can be written as a function of the latent heat L and the surface tension σ

$$S_3 = \frac{16\pi}{3} \frac{\sigma(T_c)^3}{L(T_c)^2} \frac{T_c^2}{(T_c - T)^2},$$

The ratio $S_3(T_p)/T_p$ is typically a number $\mathcal{O}(150)$ for phase transitions around the electroweak scale. From this we infer that

$$T_c - T_p \approx \sqrt{\frac{16\pi\sigma^3 T_c}{3L^2 \cdot \mathcal{O}(150)}},$$

and the inverse duration $\tilde{\beta}$ follows as

$$\tilde{\beta} = T \left. \frac{d}{dT} \frac{S_3(T)}{T} \right|_{T=T_p} \approx \mathcal{O}(10^3) \frac{T_c^{1/2} L}{\sigma^{3/2}}.$$

$\tilde{\beta}$ stems from the competition between the surface tension and latent heat.